How erosive are submarine landslides?

Harya D. Nugraha[1,2,*], Christopher A-L. Jackson[1], Howard D. Johnson[1], David M. Hodgson[3] and Michael A. Clare[4]

[1]Basins Research Group (BRG), Department of Earth Science and Engineering, Imperial College, London SW7 2BP, UK

[2]Department of Geological Engineering, Universitas Pertamina, Jakarta 12220, Indonesia

[3]School of Earth and Environment, University of Leeds, Leeds LS2 9JT, UK

[4]National Oceanography Centre, Southampton SO14 3ZH, UK

*E-mail: harya.nugraha14@imperial.ac.uk

ABSTRACT

Submarine landslides are ubiquitous on continental margins worldwide. They can pose a major hazard through triggering tsunami and can damage essential seabed infrastructure. Although slide volume, which can change through time due to substrate entrainment, is a key parameter in offshore hazard assessment, we have a poor understanding however of how erosive submarine landslides can be. Here, we use a novel method to quantify erosion, by determining the ratio of deposited (Vd) to initially evacuated (Ve) slide volumes. Slides that gain volume (i.e. erode) equate to a ratio of Vd/Ve>1. We demonstrate this method by analysing 3D seismic reflection datasets that include the recent Gorgon Slide (500 km^3), offshore NW Australia, before determining Vd/Ve ratios for other large slides worldwide. Nine of the 11 published slides have Vd/Ve>1 (median value=2), showing that emplaced slide volumes are typically larger than the initial failed volume, confirming the erosivity of their parent flows. The Gorgon Slide is the most erosive submarine landslide currently documented, having 'bulked up' by an order of magnitude (Vd/Ve=12). We

suggest its strongly erosive nature is related to the carbonate ooze substrate, which dramatically lost strength under loading. This new approach to quantifying erosion is important for geohazard assessments as substrate—flow interactions control slide speed and run-out distance. Our new insights into variations in slide volume have important implications for seabed infrastructure impact assessments and should enable more robust tsunami modelling.

INTRODUCTION

Submarine landslides (hereafter “slides”) are key components of many deep-water successions, with individual deposits covering areas >100 km^2 and comprising volumes >10,000 km^3 (e.g. Moscardelli and Wood, 2016). These slides can be tsunamigenic, such as in Papua New Guinea where a slide triggered a tsunami that killed >2000 people (Tappin et al., 2001). Slides can also damage critical seabed infrastructure, such as the global network of telecommunication cables (Carter et al., 2014), and oil and gas pipelines (e.g. Randolph and White, 2012). To date, most studies have focused on siliciclastic slides (e.g. see synthesis by Moscardelli and Wood, 2016), yet, carbonate ooze occupies a significant portion (c.30%) of the world’s ocean floor (see Appendix DR1, Dutkiewicz et al., 2015). Such carbonate oozes are known to behave differently to siliciclastic sediments, so how do these differences affect slide dynamics? The post-failure shear strength of carbonate ooze can be as low as 10% of its original strength, compared to 55% for siliciclastic clay (Gaudin and White, 2009). Slides involving or being transported over ooze-dominated seafloor may thus be more erosive (Winterwerp et al., 2012). It is therefore important to investigate how carbonate slides behave to better understand their potential impact on offshore infrastructure and their tsunamigenic potential.

During transport, a slide can be detached from its underlying substrate by a thin lubricating layer at the base of flow, i.e. hydroplaning (e.g. Mohrig et al., 1998). In this case, slide transport and emplacement will result in no erosion, and even volume loss due to partial flow transformation from debris flow to turbidity current (e.g. Sun et al., 2018). However, three-dimensional seismic reflection data provide compelling evidence that substrate deformation and entrainment is a common process, leading slides to gain volume during transport. Indicators of substrate erosion and deformation include grooves and striations (e.g. Gee et al., 2005), ramps and flats (e.g. Bull et al., 2009), downslope-diverging peel-back scours (e.g. Sobiesiak et al., 2018), and megaclasts of substrate within debrites (e.g. Hodgson et al., 2018). Despite widespread evidence for erosion, the degree of substrate entrainment during slide emplacement is poorly constrained, at least partly because of the limited exposure of exhumed slides in the field, and poor imaging by and/or limited coverage of subsurface data (e.g. seismic reflection data). Quantifying erosivity is important because: 1) entrained material during transport through basal erosion could modify slide speed and run-out distance, two key parameters for both tsunami modelling and impact assessments on submarine infrastructures (e.g. Bruschi et al., 2006); and 2) initial failed volume is a key parameter in tsunami modelling (e.g. Murty, 2003).

Here, we use 3D seismic reflection data from the Exmouth Plateau, offshore NW Australia, to quantify the erosivity of the Gorgon Slide (Fig. 1). This study focuses on the discrepancy between the volumes of evacuated (Ve) and deposited (Vd) sediments. A new measure, the Vd/Ve ratio, is introduced as a first-order estimate to quantify slide erosivity, where Vd/Ve>1 indicates substrate entrainment during transport (see Dataset and Methods). In addition, we also analyse other slides for which Vd and Ve are documented (e.g. Moscardelli and Wood, 2016). Our approach allows us to gain insights into overall physical processes occurring during the transport processes of slides and help us improve our ability to accurately assess the threat they pose to seabed infrastructure and to better constrain tsunami triggering models.

GEOLOGICAL SETTING

The Exmouth Plateau formed due to multiple rifting events, which commenced in the Late Jurassic and continued into the Early Cretaceous (Fig. 1A) (Longley et al., 2002). Post-rift deposition has been dominated by carbonates since the Late Cretaceous (Apthorpe, 1988). Miocene collision of the Australian Plate with the Eurasia and Pacific plates triggered structural inversion, promoting slope steepening across the plateau and present-day shelf (Keep et al., 1998). High fluid pressures and seismic shaking associated with this structural inversion both primed and triggered slope failure, and the emplacement of multiple slides across the plateau (e.g. Scarselli et al., 2013). Here we focus on the most recent slide, known as the Gorgon Slide (Fig. 1B-C).

DATASET AND METHODS

We analyse five 3D seismic reflection datasets (Fig. 1) that image both the evacuation and deposition zones of the Gorgon Slide and the adjacent, unfailed continental slope (Fig. 1B-C). Given a near seabed sediment velocity of 1824 m/s, and dominant frequency of 40-60 Hz, the estimated vertical resolution at the base of the Gorgon Slide (c.500 m below seabed) ranges from 8-11 m, with the 3D volumes having bin spacings of 12.5 x 18.75 m and 20 x 25 m (see Appendix DR2 for details). The present seabed and base of the Gorgon Slide (see Fig. 1D-E) were converted from time to depth using average water velocity (1519 m/s) and average near seabed sediments velocity (1824 m/s), respectively (Appendix DR2). Ten industry wells constrain the water velocity (Fig. 1B). Well ODP 762, located c.200 km NW of our seismic datasets, penetrated a similar seismic stratigraphic sequence to that encountered in the study area; we therefore used data from this well to infer near seabed lithology and its physical properties (e.g. velocity and porosity; Fig. 1A).

We calculate the ratio between the volume of the slide source or evacuated area (Ve) and the slide itself (Vd) to derive a first-order estimation of slide erosivity (Fig. DR3A). When Vd/Ve<1, we infer the slide loses volume during transport; this could reflect partial flow transformation from debris flow to turbidity current, resulting in turbidite deposition beyond the slide pinchout (Fig. DR3B). When Vd/Ve=1, we infer no net volume change from the initial failed mass (i.e. no volume addition via erosion along the basal-shear surface and/or volume loss due to flow transformation; alternatively, both can occur, but are in balance) (Fig. DR3C). Finally, Vd/Ve>1 indicates net volume gain during transport, suggesting lengthening and/or deepening of the basal-shear surface was accompanied by substrate entrainment (Fig. DR3D).

We calculated the Vd/Ve ratio for the Gorgon Slide using three established volume calculation methods (theoretical, bulk, and compacted volume; see Appendix DR4 for details). The theoretical volume method assumes that Ve and Vd have a wedge-shaped (McAdoo et al., 2000) and half-ellipsoid geometry (e.g. Wilson et al., 2004), respectively. The bulk volume method estimates Ve by calculating the volume between present-day and interpreted pre-failure seabed within the evacuation zone, while Vd is obtained by calculating the volume of the deposit between the basal-shear surface and the top surface (e.g. Piper et al., 1997). The compacted volume method takes a similar approach to the bulk volume method, but counts only the solid-state sediment fraction, removing water and pore-space (i.e. theoretical zero-porosity) (e.g. Lamarche et al., 2008). Despite the uncertainties associated with each method (Appendix DR4), Vd/Ve ratio provides a first-order estimation of slide erosivity.

EROSIVITY OF SUBMARINE LANDSLIDES

The Gorgon Slide

The source area for the Gorgon Slide is defined on its updip margin by a steep headwall scarp. The slide was transported north-westwards through an evacuation zone and accumulated in a downdip deposition zone (Fig. 1D). The slide is c.30 km-wide, with a total run-out distance of c.70 km. The slide deposit covers a total area of 1760 km^2 and thickens downslope to c.500 m. Transparent and chaotic seismic reflections likely reflect the debritic material forming the slide matrix (Fig. 1D-E) (e.g. Posamentier and Martinsen, 2011). Packages of subparallel, high-amplitude reflections encased in the interpreted debrite are interpreted as megaclasts (Fig. 1E) (e.g. Jackson, 2011; Hodgson et al., 2018), either sourced from the headscarp or entrained from the substrate. Basal erosion is evidenced by truncation of underlying seismic reflections (Fig. 1E).

The Vd of the Gorgon Slide was calculated using the basal-shear surface and seabed (see Fig. 1D-E). As a small part (c.7%) of the Gorgon Slide is not imaged within the 3D seismic reflection data (i.e. 166 km^2 of 1760 km^2, see Fig. 1C), the calculated Vd is a minimum value. Ve was estimated by using the adjacent unfailed slope as a proxy for the pre-failure physiography across the evacuation zone (Fig. 2). The estimated Vd/Ve ratios of the Gorgon Slide range from 5-12, depending on the calculation method (see Appendix DR5). Critically, all methods suggest the Gorgon Slide was strongly erosive (i.e. Vd/Ve>1), an observation consistent with the abundant evidence for seismic-scale erosion along the basal-shear surface.

Global Trend of Submarine Landslides Erosivity

In order to place our results in a global context, we collated geometrical data from other slides (see Appendix DR6). Of the 357 slides documented in 97 papers, only 11 had data on both Ve and Vd. Our analysis shows that 9 of the 11 published slides are erosive, having Vd/Ve>1, with a median value of 2 (Fig. 3). On average, the Vd/Ve of the documented slides suggests that the final preserved slide volume can be three times the initial failed volume. The Gorgon Slide has a Vd/Ve ratio of up to 12 (and a conservative estimate of 5), making it the most erosive slide yet documented (Fig. 3B).

Although most are erosive, two slides display Vd/Ve<1 (Fig. 3B): 1) in the South China Sea, where volume loss is attributed to partial flow transformation to a turbidity current resulting in deposition of (sub-seismic) turbidites beyond the main slide pinchout, and pore volume reduction due to continuous shearing during transport (i.e. shear compaction) (Sun et al., 2018); and 2) in New Zealand, the Ruatoria Debris Avalanche, where the evacuation zone was formed by a combination of slope failure and tectonic erosion due to seamount subduction (i.e. not solely related to flow processes during transport) (Collot et al., 2001).

DISCUSSION

Large submarine landslides are predominantly erosive

Our results show that the volumes of most slides are larger than the initial failed volume, thereby confirming the erosivity of their parent flows (Fig. 3). Substrate entrainment and volume gain occurs because the shear stress exerted by the overriding parent flow exceeded the shear strength of the substrate. The overriding flow may elevate shallow subsurface pore pressures, causing liquefaction or strain softening (e.g. Ortiz-Karpf et al., 2017), or substrate deformation (e.g. Butler and McCaffrey, 2010). Both mechanisms will reduce the strength of the substrate, making it susceptible to entrainment. Substrate entrainment could also occur due to tooling by rigid blocks (e.g. megaclasts); this process forms tool marks, such as grooves and striations (e.g. Gee et al., 2005).

We suggest that the Gorgon Slide was strongly erosive because of the specific properties of the carbonate ooze substrate. Carbonate ooze is dominated by fragile foraminifera and nannofossils, which become weakly cemented at their contacts during early burial; this preserves higher-than-normal near-surface porosities and results in higher initial strength than (uncemented) siliciclastic sediments (von Rad et al., 1992). Under loading, these fragile biogenic particles are crushed, generating excess near-seabed pore pressures, and causing a dramatic loss of strength (e.g. Sharma and Joer, 2015). When carbonate oozes failed, their residual strength can be only 10% of their initial strength; the residual strength of these materials is significantly lower than that of siliciclastic sediments (i.e. 55%, see Appendix DR7, Gaudin and White, 2009).

In contrast, volume loss during transport could occur due to entrainment of coarse-grained (e.g. sandy) sediments by the flow (e.g. Dykstra et al., 2011), and/or ingestion of water into the flow (e.g. Talling et al., 2012). For example, Sun et al. (2018) document a median volume loss of 86 km^3 (c.13.6% of Vd) for a slide in the South China Sea. They relate this volume discrepancy to flow transformation from the slide (debris flow) into slide-generated turbidity currents. In addition, continuous shearing during transport may have added to volume loss, as pore volume will be reduced even when small shear stresses are applied to fine-grained sediments (Piper et al., 1997).

Implications of submarine landslides erosivity for geohazards assessments

Vd/Ve ratio provides a first-order, quantitative estimate of whether a slide increases or decreases its volume during transport. When a slide is erosive and bulks-up, its transport speed may decrease due to enhanced basal friction, thereby reducing run-out distance (e.g. Puzrin, 2016; Schulz et al., 2009). Similarly, when a slide experiences minimal erosion and/or hydroplanes, both its transport speed and run-out distance may increase (e.g. Mohrig et al., 1998). These two factors, slide speed and run-out distance, are key components for both tsunami modelling (e.g. Murty, 2003), and for assessing the potential impact slides may have on seabed infrastructures (e.g. Bruschi et al., 2006). In addition, Ve is a key factor for tsunami modelling, as it dictates how much overlying water is displaced during failure (e.g. Murty, 2003). Accurate volume assessment is especially challenging if only Vd is known, and if there is significant erosion or partial flow transformation. For example, the use of Vd as an estimate of Ve for tsunami modelling will overestimate displacement of the overlying water when $Vd/Ve>1$. Similarly, if $Vd/Ve<1$, tsunami modelling will underestimate the displacement of the overlying water. Therefore, to understand uncertainties associated with tsunami modelling, a range of Vd/Ve scenarios should be considered. Our study suggests that most slides are erosive, and that under-represented carbonate slides, such as the Gorgon Slide, could be more erosive than siliciclastic slides. Vd/Ve ratio is useful as a first-order estimate to understand slides erosivity and could also be used as a tool for geohazards risk assessments.

ACKNOWLEDGEMENTS

We thank Geoscience Australia for providing seismic and borehole data. Schlumberger are thanked for providing software (Petrel) to Imperial College. The first author thanks the Indonesia Endowment Fund for Education (LPDP) (Grant No.: 20160822019161) for its financial support. MC was supported by the NERC National Capability CLASS Programme [Climate Linked Atlantic Sector Science Programme (No. NE/R015953/1)].

REFERENCES CITED

Apthorpe, M., 1988, Cainozoic depositional history of the North West Shelf: The North West Shelf, Australia: Petroleum Exploration Society of Australia, p. 55-84.

Bruschi, R., Bughi, S., Spinazzè, M., Torselletti, E., and Vitali, L., 2006, Impact of debris flows and turbidity currents on seafloor structures: Norwegian Journal of Geology/Norsk Geologisk Forening, v. 86, no. 3.

Bull, S., Cartwright, J., and Huuse, M., 2009, A review of kinematic indicators from mass-transport complexes using 3D seismic data: Marine and Petroleum Geology, v. 26, no. 7, p. 1132-1151.

Butler, R., and McCaffrey, W., 2010, Structural evolution and sediment entrainment in mass-transport complexes: outcrop studies from Italy: Journal of the Geological Society, v. 167, no. 3, p. 617-631.

Carter, L., Gavey, R., TALLING, P. J., and Liu, J. T., 2014, Insights into submarine geohazards from breaks in subsea telecommunication cables: Oceanography, v. 27, no. 2, p. 58-67.

Collot, J. Y., Lewis, K., Lamarche, G., and Lallemand, S., 2001, The giant Ruatoria debris avalanche on the northern Hikurangi margin, New Zealand: Result of oblique seamount subduction: Journal of Geophysical Research: Solid Earth, v. 106, no. B9, p. 19271-19297.

Dutkiewicz, A., Müller, R. D., O'Callaghan, S., and Jónasson, H., 2015, Census of seafloor sediments in the world's ocean: Geology, v. 43, no. 9, p. 795-798.

Dykstra, M., Garyfalou, K., Kertznus, V., Kneller, B., Milana, J. P., Molinaro, M., Szuman, M., and Thompson, P., 2011, Mass-transport deposits: Combining outcrop studies and seismic forward modeling to understand lithofacies distributions, deformations, and their seismic stratigraphic expression: SEPM Special Publication, v. 96, p. 293-310.

Gaudin, C., and White, D., 2009, New centrifuge modelling techniques for investigating seabed pipeline behaviour, *in* Proceedings 17th International Conference on Soil Mechanics and Geotechnical Engineering, Alexandria, 2009, p. 448-451.

Gee, M., Gawthorpe, R., and Friedmann, J., 2005, Giant striations at the base of a submarine landslide: Marine Geology, v. 214, no. 1, p. 287-294.

Hodgson, D., Brooks, H., Ortiz-Karpf, A., Spychala, Y., Lee, D., and Jackson, C.-L., 2018, Entrainment and abrasion of megaclasts during submarine landsliding and their impact on flow behaviour: Geological Society, London, Special Publications, v. 477, p. SP477. 426.

Jackson, C. A., 2011, Three-dimensional seismic analysis of megaclast deformation within a mass transport deposit; implications for debris flow kinematics: Geology, v. 39, no. 3, p. 203-206.

Keep, M., Powell, C., and Baillie, P., 1998, Neogene deformation of the North West Shelf, Australia: The sedimentary basins of Western Australia, v. 2, p. 81-91.

Lamarche, G., Joanne, C., and Collot, J. Y., 2008, Successive, large mass-transport deposits in the south Kermadec fore-arc basin, New Zealand: The Matakaoa Submarine Instability Complex: Geochemistry, Geophysics, Geosystems, v. 9, no. 4.

Longley, I. M., Buessenschuett, C., Clydsdale, L., Cubitt, C. J., Davis, R. C., Johnson, M. K., Marshall, N. M., Murray, A. P., Somerville, R., and Spry, T. B., 2002, The North West Shelf of Australia - a Woodside Perspective, *in* Keep, M., and Moss, S. J., eds., The Sedimentary Basins of Western Australia 3: Petroleum Exploration Society of Australia Symposium: Perth, p. 28-88.

McAdoo, B., Pratson, L., and Orange, D., 2000, Submarine landslide geomorphology, US continental slope: Marine Geology, v. 169, no. 1, p. 103-136.

Mohrig, D., Ellis, C., Parker, G., Whipple, K. X., and Hondzo, M., 1998, Hydroplaning of subaqueous debris flows: Geological Society of America Bulletin, v. 110, no. 3, p. 387-394.

Moscardelli, L., and Wood, L., 2016, Morphometry of mass-transport deposits as a predictive tool: GSA Bulletin, v. 128, no. 1/2, p. 47-80.

Murty, T., 2003, Tsunami wave height dependence on landslide volume: Pure and applied geophysics, v. 160, no. 10-11, p. 2147-2153.

Ortiz-Karpf, A., Hodgson, D. M., Jackson, C. A.-L., and McCaffrey, W. D., 2017, Influence of Seabed Morphology and Substrate Composition On Mass-Transport Flow Processes and Pathways: Insights From the Magdalena Fan, Offshore Colombia: Journal of Sedimentary Research, v. 87, no. 3, p. 189-209.

Piper, D. J. W., Pirmez, C., Manley, P. L., Long, D., Flood, R. D., Normark, W. R., and Showers, W., Mass Transport Deposits of the Amazon Fan, *in* Proceedings Ocean Drilling Program, Scientific Results1997, Volume 155, p. 109-146.

Posamentier, H. W., and Martinsen, O. J., 2011, The character and genesis of submarine mass-transport deposits: insights from outcrop and 3D seismic data: Mass-transport deposits in deepwater settings: Society for Sedimentary Geology (SEPM) Special Publication 96, p. 7-38.

Puzrin, A. M., 2016, Simple criteria for ploughing and runout in post-failure evolution of submarine landslides: Canadian Geotechnical Journal, v. 53, no. 8, p. 1305-1314.

Randolph, M. F., and White, D. J., 2012, Interaction forces between pipelines and submarine slides—A geotechnical viewpoint: Ocean Engineering, v. 48, p. 32-37.

Scarselli, N., McClay, K., and Elders, C., Submarine slide and slump complexes, Exmouth Plateau, NW Shelf of Australia, *in* Proceedings The Sedimentary Basins of Western Australia IV: Proceedings of the Petroleum Exploration Society of Australia Symposium, Perth, 2013.

Schulz, W. H., McKenna, J. P., Kibler, J. D., and Biavati, G., 2009, Relations between hydrology and velocity of a continuously moving landslide—evidence of pore-pressure feedback regulating landslide motion?: Landslides, v. 6, no. 3, p. 181-190.

Sharma, S., and Joer, H., Some characteristics of carbonate sediments from NorthWest Shelf, Western Australia, *in* Proceedings Frontiers in Offshore Geotechnics III: Proceedings of the 3rd International Symposium on Frontiers in Offshore Geotechnics (ISFOG 2015)2015, Volume 1, Taylor & Francis Books Ltd, p. 1109-1114.

Sobiesiak, M. S., Kneller, B., Alsop, G. I., and Milana, J. P., 2018, Styles of basal interaction beneath mass transport deposits: Marine and Petroleum Geology, v. 98, p. 629-639.

Sun, Q., Alves, T., Lu, X., Chen, C., and Xie, X., 2018, True volumes of slope failure estimated from a Quartenary mass-transport deposit in the northern South China Sea: Geophysical Research Letters.

Talling, P. J., Masson, D. G., Sumner, E. J., and Malgesini, G., 2012, Subaqueous sediment density flows: Depositional processes and deposit types: Sedimentology, v. 59, no. 7, p. 1937-2003.

Tappin, D., Watts, P., McMurtry, G., Lafoy, Y., and Matsumoto, T., 2001, The Sissano, Papua New Guinea tsunami of July 1998—offshore evidence on the source mechanism: Marine Geology, v. 175, no. 1-4, p. 1-23.

Ten Brink, U. S., Geist, E. L., and Andrews, B. D., 2006, Size distribution of submarine landslides and its implication to tsunami hazard in Puerto Rico: Geophysical Research Letters, v. 33, no. 11.

von Rad, U., Haq, B. U., Kidd, R. B., and O'Connell, S. B., 1992, Proceedings of the Ocean Drilling Program, Scientific Results, College Station, TX, Ocean Drilling Program.

Wilson, C. K., Long, D., and Bulat, J., 2004, The morphology, setting and processes of the Afen Slide: Marine Geology, v. 213, no. 1-4, p. 149-167.

Winterwerp, J., Kesteren, W., Prooijen, B., and Jacobs, W., 2012, A conceptual framework for shear flow–induced erosion of soft cohesive sediment beds: Journal of Geophysical Research: Oceans, v. 117, no. C10.

FIGURE CAPTIONS

Figure 1. A: Location of study area (EP: Exmouth Plateau; AR: Argo Abyssal Plain; GA: Gascoyne Abyssal Plain; CU: Cuvier Abyssal Plain). Yellow dot = location of ODP 762. B: Seabed time-structure map (top Gorgon Slide) showing slide evacuation and deposition zones. Red dots = wells used for depth conversion. C: Extent of the Gorgon Slide (grey). Black dashed line defines the seismic-scale pinchout of the slide; c. 7% of the slide is not imaged by 3D seismic data but is mapped on 2D seismic profiles (green lines). Gorgon, Acme, Draeck, Duyfken, and Io-Jansz are the 3D seismic datasets were used in this study. D: NW-trending depositional dip-oriented seismic profile across the Gorgon Slide, showing cross-sectional view of the evacuation and deposition zones. E: NE-trending depositional strike seismic profile across the Gorgon Slide. Locations of seismic profiles are shown in B and C.

Figure 2. A: NW-trending seismic profile across the unfailed margin, just SW of the headwall of the Gorgon Slide. B: Seabed time-structure map showing the headwall of the Gorgon Slide and the adjacent unfailed margin to the SW. C: NW-trending seismic profile across the headwall of the Gorgon Slide and the reconstructed (i.e. pre-failure) seabed. D: Reconstructed pre-failure seabed time-structure map.

Figure 3. A: World distribution of documented slides in peer-reviewed literature, containing information on evacuated (Ve) and deposited (Vd) volumes. Note that the Gorgon Slide as the only carbonate-domainted slide. B: Vd/Ve ratio of the submarine landslide in (A).

Figure 1

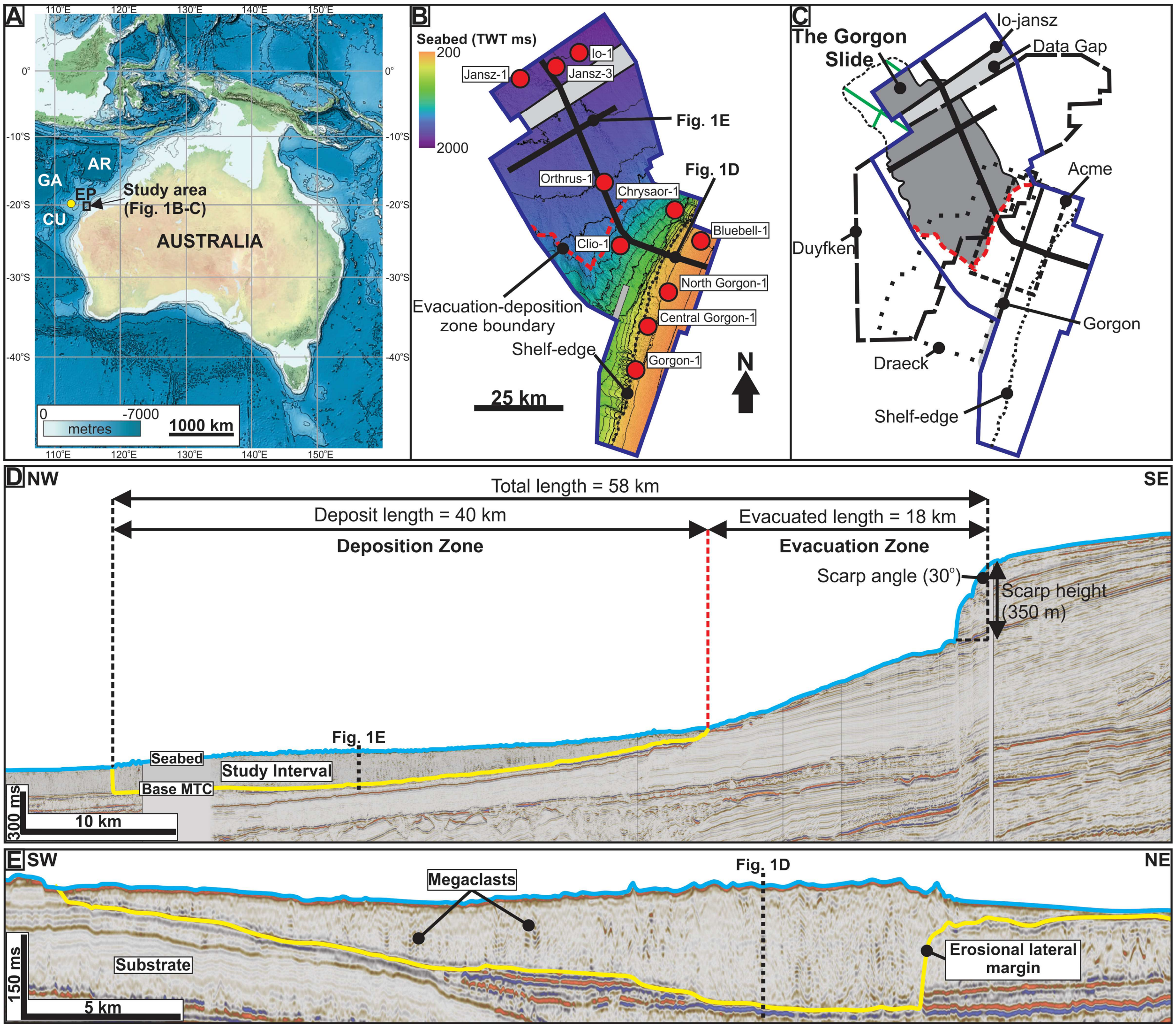

A
AR
GA
EP
CU
Study area
(Fig. 1B-C)
AUSTRALIA
0
-7000
metres
1000 km
B
Seabed (TWT ms)
200
2000
Io-1
Jansz-1
Jansz-3
Fig. 1E
Fig. 1D
Orthrus-1
Chrysaor-1
Bluebell-1
Clio-1
North Gorgon-1
Central Gorgon-1
Gorgon-1
Evacuation-deposition
zone boundary
Shelf-edge
25 km
N
C
The Gorgon
Slide
Io-jansz
Data Gap
Acme
Duyfken
Gorgon
Draeck
Shelf-edge
D NW
SE
Total length = 58 km
Deposit length = 40 km
Evacuated length = 18 km
Deposition Zone
Evacuation Zone
Scarp angle (30°)
Scarp height
(350 m)
Fig. 1E
Seabed
Study Interval
Base MTC
300 ms
10 km
E SW
NE
Fig. 1D
Megaclasts
Substrate
Erosional lateral
margin
150 ms
5 km

319 Figure 2

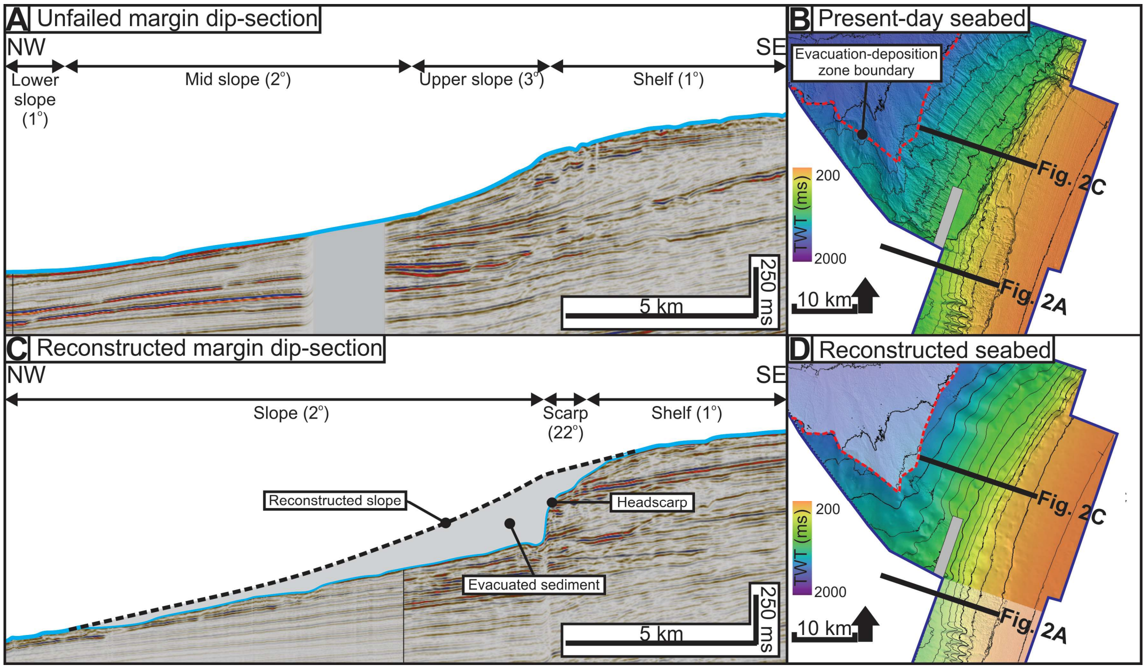

320

321 Figure 3

322